

Network Controllability in Transmodal Cortex Predicts Positive Psychosis Spectrum Symptoms

Linden Parkes, Tyler M. Moore, Monica E. Calkins, Matthew Cieslak, David R. Roalf, Daniel H. Wolf, Ruben C. Gur, Raquel E. Gur, Theodore D. Satterthwaite, and Danielle S. Bassett

ABSTRACT

BACKGROUND: The psychosis spectrum (PS) is associated with structural dysconnectivity concentrated in transmodal cortex. However, understanding of this pathophysiology has been limited by an overreliance on examining direct interregional connectivity. Using network control theory, we measured variation in both direct and indirect connectivity to a region to gain new insights into the pathophysiology of the PS.

METHODS: We used psychosis symptom data and structural connectivity in 1068 individuals from the Philadelphia Neurodevelopmental Cohort. Applying a network control theory metric called average controllability, we estimated each brain region's capacity to leverage its direct and indirect structural connections to control linear brain dynamics. Using nonlinear regression, we determined the accuracy with which average controllability could predict PS symptoms in out-of-sample testing. We also examined the predictive performance of regional strength, which indexes only direct connections to a region, as well as several graph-theoretic measures of centrality that index indirect connectivity. Finally, we assessed how the prediction performance for PS symptoms varied over the functional hierarchy spanning unimodal to transmodal cortex.

RESULTS: Average controllability outperformed all other connectivity features at predicting positive PS symptoms and was the only feature to yield above-chance predictive performance. Improved prediction for average controllability was concentrated in transmodal cortex, whereas prediction performance for strength was uniform across the cortex, suggesting that indexing indirect connections through average controllability is crucial in association cortex.

CONCLUSIONS: Examining interindividual variation in direct and indirect structural connections to transmodal cortex is crucial for accurate prediction of positive PS symptoms.

<https://doi.org/10.1016/j.biopsych.2021.03.016>

The psychosis spectrum (PS) is broadly characterized by positive (e.g., hallucinations, delusions) and negative (e.g., avolition, social withdrawal) psychosis symptoms (1). The PS follows a continuous distribution of severity, with absence of these symptoms at one end and disorders such as schizophrenia at the other (2,3). Transition along the PS toward schizophrenia occurs predominantly during adolescence and young adulthood (2,4) and is thought to be underpinned by widespread structural dysconnectivity that emerges during this time (5–7). In this context, regional (dys)connectivity is typically characterized by examining the direct connections between regions. However, mounting evidence demonstrates that any region's capacity to affect the activity of other brain regions is also influenced by the presence of indirect connections (8–15). How these indirect aspects of structural connectivity—and their impact on the spread of activity and control of brain states—relate to PS symptoms remains unclear, rendering our understanding of the neurobiology of the PS incomplete.

The capacity for spatially distributed brain regions to communicate and coordinate their activity is essential for

normal cognitive and affective functions (11). Critical to this communication is the brain's underlying structural connectivity, which provides a scaffold along which activity in one region can spread to, and influence, another. A brain region's connectivity profile is often summarized regionally using graph-theoretic metrics such as degree and strength (16); the former is calculated by counting the number of binary direct connections to a region, and the latter by summing over the weights of those connections. These metrics have aided our understanding of the brain's structural organization (7,17,18). For example, adolescent development gives rise to regions with disproportionately high degree and strength, known as hubs (19–21). In cerebral cortex, hubs are commonly found in transmodal association areas (20,22–24), where they are thought to integrate across functionally specialized and segregated subnetworks enabling complex higher-order functions (22,25–27). In support of this integrative role, transmodal regions connect with far-reaching and cascading indirect pathways that exert regulatory control over unimodal regions (28–30). However, these indirect paths are not captured by the analysis of regional strength. Given that these

indirect pathways converge to a greater extent on transmodal regions than unimodal regions (28,31), assessing variation in indirect connection pathways is likely critical to understanding the integrative role of association cortex.

The literature has also begun to reveal how structural connectivity varies along the PS (32–37). Notably, dysconnectivity in transmodal cortex is a prominent feature in individuals on the PS. Transmodal dysconnectivity is reported in schizophrenia (35,37–40) as well as the early clinical stages of psychosis (34) and is thought to reflect disrupted integration in the brain (22,41,42). In addition, white matter integrity studies have shown that individuals at ultra-high risk for psychosis as well as patients with first-episode psychosis show abnormalities in the long association fibers that route information between transmodal cortex and the rest of the brain (32). However, these studies (34,35,37–40) have examined white matter connectivity in the absence of an explicit model of how the brain's complex topology facilitates the spread of activity along indirect pathways. Without such a model, studies may potentially miss important symptom-related variation in regional connectivity profiles, which may be particularly important in transmodal cortex (28,31). Thus, examining dysconnectivity along the complex indirect pathways that stem from transmodal cortex may help elucidate the pathophysiology of the PS.

Here, we use network control theory (NCT) (9) to examine whether individuals on the PS display alterations in the ability of indirect structural connections to influence the spread of activity and control brain states. NCT is a branch of physical and engineering sciences that treats a network as a dynamical system (9,43). Broadly, NCT models signals that originate at specific control points and that move through the network to influence changes in system state. In the brain, NCT models each region's activity as a time-dependent internal state that is predicted from a combination of three factors: 1) its previous state, 2) whole-brain structural connectivity, and 3) external inputs. In its simplest form, NCT assumes that brain dynamics are macroscopically linear. While this assumption is false at the microscopic level (e.g., single neuron), recent work has shown that linear models of dynamics outperform nonlinear models when predicting the macroscopic brain activity measured by functional magnetic resonance imaging (44). Thus, despite their simplicity, linear models of dynamics provide a good proxy for the kinds of brain activity often studied in psychiatry research. After linearizing the system's dynamics, average controllability quantifies a region's capacity to distribute activity throughout the brain, beyond the bounds of its direct connections, to guide changes in brain state (9,43). Average controllability increases throughout development (45), supporting optimal executive function (46,47), and is disrupted in bipolar disorder (48). Critically, while high strength is necessary for high average controllability (9), analysis of interindividual differences has shown that strength and average controllability have unique variance over subjects and thus do not represent redundant summaries of structural connectivity (46). However, it remains unclear to what extent interindividual variability in average controllability predicts interindividual differences in PS symptoms.

Here, we sought to understand how variance in direct and indirect connections to a region differentially contribute to the prediction of PS symptoms. We operationalized this goal by comparing the ability of strength and average controllability to predict positive and negative PS symptoms in out-of-sample testing (49). We tested three hypotheses. First, owing to its capacity to use both direct and indirect structural connections to control brain states, we hypothesized that average controllability, not strength, would best predict PS symptoms. Second, owing to their far-reaching indirect connectivity profiles (10,31), we hypothesized that regions in transmodal cortex would be more sensitive to variations in indirect connectivity compared with regions in unimodal sensorimotor cortex. Thus, we predicted that regional cross-subject correlations between strength and average controllability would be lower in transmodal cortex than in unimodal cortex. Reflecting this divergence in transmodal cortex, we expected that better predictive performance for average controllability, compared with strength, would be driven predominantly by regions in transmodal cortex. Finally, we examined the extent to which our results were specific to average controllability by comparing against the following graph-theoretic measures of centrality that also index indirect connections: betweenness centrality, closeness centrality, and subgraph centrality (17).

METHODS AND MATERIALS

Participants

Participants included 1068 individuals from the Philadelphia Neurodevelopmental Cohort (50), a community-based study of brain development in youths aged 8 to 22 years with a broad range of psychopathology (51,52). See [Supplemental Methods](#) for details.

Dimensional Measures of the PS

To study interindividual variation in the PS, we used a model of psychopathology based on the *p*-factor hypothesis (49,53) (see [Supplement](#) for details). We quantified three orthogonal dimensions of psychopathology: psychosis-positive, which represented the positive domain of the PS; psychosis-negative, which represented the negative domain of the PS; and overall psychopathology, which represented individuals' tendency to develop all forms of psychopathology. The joint examination of these three dimensions allowed us to examine the extent to which dysconnectivity reflected PS-specific or disorder-general biomarkers.

Structural Network Estimation

For details on image acquisition, quality control, and processing, see [Supplemental Methods](#). For each participant, deterministic fiber tracking was conducted, and the number of streamlines intersecting region *i* and region *j* in a parcellation of *N* = 200 regions (54) was used to weight the edges of an undirected adjacency matrix, *A*.

Strength

A simple summary of a region's direct connections to the rest of the brain is its weighted degree, or strength (16). Within each

Network Controllability Predicts the Psychosis Spectrum

participant's A matrix, we calculated strength s for region i as the sum of edge weights over all regions in the network:

$$s_i = \sum_{j=1}^N A_{ij}. \quad (1)$$

Network Controllability

NCT provides a means to study how the brain's structural network supports, constrains, and controls temporal dynamics in brain activity. Details of the NCT tools and their application have been extensively discussed in previous work (9,10,43,46,47,55–57). The application of NCT in neuroscience has been diverse. For example, NCT has been shown to assist in detecting neurons critical to locomotion in *Caenorhabditis elegans* (58). In addition, human work has shown that brain state transitions induced via direct electrical stimulation, and measured by electrocorticography data, correlate to state transitions predicted from NCT (56). These works illustrate the capacity of NCT to use a network's underlying structural topology to make meaningful predictions about its function. Here, we draw on an NCT metric known as average controllability (9,45). Below, we describe the derivation of average controllability and the model of population activity that underpins it.

We define the activity state of the brain using a simplified noise-free linear discrete-time and time-invariant model of regional dynamics:

$$x(t+1) = Ax(t) + B_\kappa u_\kappa(t), \quad (2)$$

where $x(t)$ is a $N \times 1$ vector that represents the state of the system at time t . Here, N is the number of brain regions; thus, the state is the pattern of brain activity across these regions at a single point in time. Over time, $x(t)$ denotes the brain state trajectory, a temporal sequence of the aforementioned pattern of brain activity. The matrix A denotes the normalized $N \times N$ adjacency matrix. We normalized each participant's A matrix in the following manner:

$$A = \frac{A}{|\lambda(A)|_{\max} + c}. \quad (3)$$

Here, $|\lambda(A)|_{\max}$ is the largest eigenvalue of A and $c = 1$ to ensure system stability (see Supplemental Methods).

The matrix B_κ in equation 2 is of size $N \times N$ and describes the brain regions κ into which we inject activity before assessing the impulse response of the system. We calculated average controllability for each brain region separately; thus, B_κ simplifies to an $N \times 1$ vector where the element corresponding to the region being assessed is set to 1 and all other elements are set to 0. Finally, $u_\kappa(t)$ is an $N \times 1$ vector that encodes the magnitude of the activity that we inject into a given brain region before observing the impulse response. Here, this magnitude is set to 1. Note, this magnitude value is arbitrary, and setting it to any other nonzero value would not affect the variance in average controllability over participants.

Average Controllability

Average controllability describes the ability of a network to spread the activity injected into a control node throughout the

system to affect changes in brain state (9). Regions with high average controllability are thought to be capable of switching the brain between easy-to-reach states using low amounts of energy. As in previous work, we used $\text{Trace}(W_{\kappa,T})$, where $W_{\kappa,T}$ is the controllability Gramian,

$$W_{\kappa,T} = \sum_{\tau=0}^{T-1} A^\tau B_\kappa B_\kappa^\top (A^\top)^\tau, \quad (4)$$

where \top denotes the transpose operation, τ indicates the time step of the trajectory, and T denotes the time horizon, which is set to infinity. Average controllability is computed for each node in A separately.

Average controllability is not the only way to probe indirect connections to a region. To examine the extent to which our results were specific to average controllability, we included three additional graph-theoretic measures of centrality that also characterize indirect connections to a region (17), albeit in the absence of a dynamical model. These metrics were 1) betweenness centrality, 2) closeness centrality, and 3) subgraph centrality. For extended discussion and definition of these metrics, see the Supplement and (17).

Machine Learning Prediction

The above procedures generated five 1068×200 matrices (X) of regional structural connectivity features: strength (X_s) (Figure 1A), average controllability (X_a) (Figure 1A), betweenness centrality (X_{bc}), closeness centrality (X_{cc}), and subgraph centrality (X_{sgc}). To ensure normality, columns of these matrices, as well as the PS symptom dimensions, were normalized using an inverse normal transformation (59,60). Then, connectivity features were each taken as multivariate input features to a nonlinear kernel ridge regression (61) to predict symptom dimensions (y) in a series of prediction models. Prediction models were scored using out-of-sample root-mean-squared error (RMSE) and the correlation between true and predicted y (hereafter, accuracy) and are explained in full in the Supplemental Methods. Briefly, our prediction models collectively examined 1) how prediction performance for a given y varied over X (Figure 1B, primary prediction model; Figure S1, secondary prediction model), 2) whether prediction performance for a specific (X,y) combination exceeded chance levels (Figure S2, null prediction model), and 3) how prediction performance varied as a function of the principal cortical gradient of functional connectivity that separates transmodal cortex from unimodal cortex (25) (Figure 1C, binned-regions prediction model).

Characterizing the Unique Interindividual Variation Introduced to Regional Connectivity Profiles Through the Examination of Indirect Connections

In addition to predicting symptom dimensions, we sought to quantify the extent to which analyzing indirect structural connections to a region revealed unique interindividual variation compared with analyzing only the direct connections to a region. We calculated the regional cross-subject Pearson's

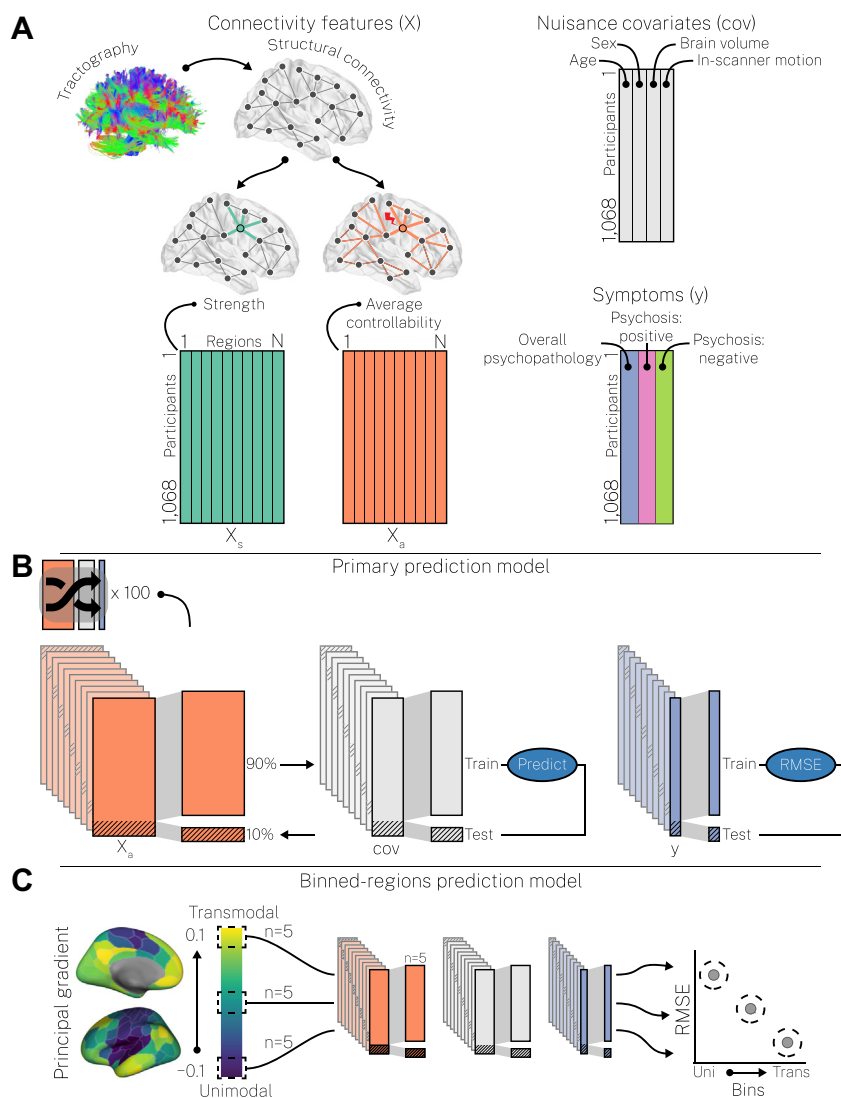


Figure 1. Machine learning prediction models. **(A)** We combined regional structural connectivity features (e.g., strength, X_s ; average controllability, X_a), nuisance covariates (cov; age, sex, total brain volume, and in-scanner motion), and symptom dimensions (y ; overall psychopathology, positive psychosis spectrum symptoms, and negative psychosis spectrum symptoms) into two main prediction models. Note, we ran each combination of X and y separately. **(B)** In our primary prediction model, X was used to predict y , controlling for age, sex, brain volume, and in-scanner motion, via 100 repeats of 10-fold cross-validation, each repeat using a different random split of the data. This model provided robust estimates of prediction performance that could be compared across combinations of X and y . This primary prediction model was supplemented with a secondary prediction model that incorporated hyperparameter optimization (see Figure S1 and the Supplement for details) and a null prediction model that assessed whether specific combinations of X and y yielded above-chance prediction performance (see Figure S2 and the Supplement for details). **(C)** In our binned-regions prediction model, X was used to predict y , controlling for age, sex, brain volume, and in-scanner motion, using nonoverlapping subsets of five regions sampled from the principal cortical gradient of functional connectivity. The principal cortical gradient (left) was generated in our data using resting-state functional connectivity (see Supplement for details). This model enabled examination of how prediction performance varied over the putative cortical hierarchy. RMSE, root-mean-squared error; trans, transmodal; uni, unimodal.

correlations between strength and average controllability in the full sample. Lower correlations indicated greater unique variance across strength and average controllability, suggesting greater influence of indirect connections to a region's connectivity profile. Then, we examined how these regional correlation values varied over the principal cortical gradient (25). We calculated the Pearson's correlation between the cortical gradient and the aforementioned cross-subject correlation maps. We assigned p values with the spin test (62–64), using 10,000 spins.

RESULTS

Participants

Sample demographics, including counts of individuals who endorsed presence of a broad array of clinical symptoms (50,51), are shown in Table 1 (see Figure S4 for mean symptom dimensions as a function of these groups).

Examining Indirect Regional Structural Connectivity With Average Controllability Enables Better Prediction of Positive PS Symptoms

First, we examined how indirect connections to a region affected predictive performance for each symptom dimension by 1) comparing RMSE and accuracy across connectivity features and 2) examining each connectivity feature's capacity to predict symptom dimensions beyond chance levels. While performance varied as a function of connectivity feature for each symptom dimension (Figure 2), only average controllability was able to predict psychosis-positive scores beyond chance levels (Figure 2A; $\ast p < .05$ false discovery rate-corrected; see Figure S8 for empirical nulls). Apart from this, betweenness and closeness centrality were the best predictors of psychosis-negative (Figure 2B), and subgraph centrality was the best predictor of overall psychopathology (Figure 2C). However, none of these predictive results were above chance. In addition, we found that our scoring metrics—RMSE and

Network Controllability Predicts the Psychosis Spectrum

Table 1. Summary of Demographic and Psychopathology Data (N = 1068)

Characteristics	Sample
Age, Years, Mean \pm SD	15.36 \pm 3.42
Sex, n (%)	
Male	485 (45.51%)
Female	582 (54.49%)
Psychopathology Categories, n (%)	
Psychosis spectrum	303 (28.37%)
Manic episode	11 (1.03%)
Major depressive episode	156 (14.01%)
Bulimia	4 (0.37%)
Anorexia	15 (1.40%)
Social anxiety disorder	261 (24.44%)
Panic	10 (0.94%)
Agoraphobia	61 (5.71%)
Obsessive compulsive	30 (2.81%)
Posttraumatic stress	136 (12.73%)
Attention-deficit/hyperactivity	168 (15.73%)
Oppositional defiant	353 (33.05%)
Conduct	85 (7.96%)

Owing to comorbidity, individual participants may be present in more than one category of lifetime prevalence.

accuracy—were highly correlated over 100 different cross-validation splits of the data ($r = 0.89 \pm 0.02$; correlations were averaged over connectivity features and symptom dimensions). Finally, the above effects were largely reproduced under our secondary prediction model (Figure S9). Thus, in partial support of hypothesis 1, our results demonstrate that summarizing both the direct and indirect properties of regional connectivity is critical for predicting positive PS symptoms.

Furthermore, this effect was selective for average controllability, suggesting that how indirect connections are summarized regionally is also important.

Variance in Indirect Structural Connections Is Increasingly Relevant in Transmodal Cortex

The above results underscored the importance of using average controllability to incorporate indirect connections into the prediction of positive PS symptoms. Next, we characterized where along the cortical gradient interindividual variation in indirect connectivity was most pronounced by correlating strength and average controllability (see Figure S10 for all combinations of connectivity features). In support of hypothesis 2, we found that regional correlations between strength and average controllability decreased as a function of the cortical gradient (Figure 3A). Specifically, regions in unimodal cortex showed the strongest correlations ($r \sim .7$), while regions in transmodal cortex showed weaker correlations ($r \sim .5$). This result offers two insights. First, while strength and average controllability are always positively correlated across the brain, those correlations are not redundant, suggesting that variance in the indirect connections captured by average controllability are relevant at all levels of the cortex. Second, regions in transmodal cortex have more complex profiles of indirect connectivity that drive greater divergence between average controllability and strength.

Indirect Connectivity From Transmodal Cortex Underpins Better Prediction Performance of Positive PS Symptoms

Having found that average controllability and strength diverged most in transmodal cortex, we tested hypothesis 3: that this divergence in transmodal cortex would drive improved performance for predicting psychosis-positive scores using

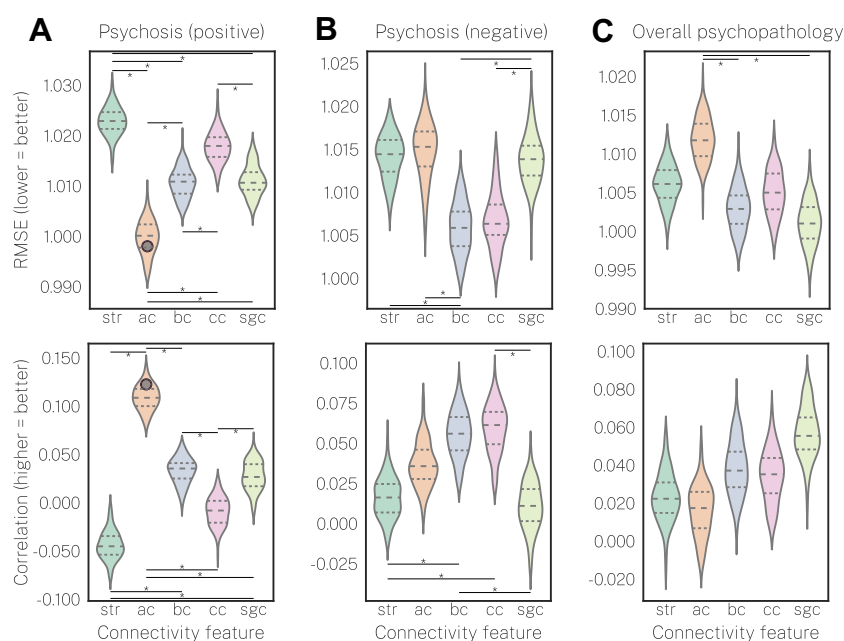


Figure 2. Average controllability is the best predictor of positive psychosis spectrum symptoms and is the only connectivity feature to predict beyond chance levels. Each subplot shows distributions of 100 estimates of prediction performance under our primary prediction model using a nonlinear kernel ridge regression estimator. The top row indicates prediction performance measured via root-mean-squared error (RMSE; lower = better), and the bottom row indicates prediction performance measured via the correlation between true y and predicted y (higher = better). Furthermore, to illustrate which (X, y) combinations yielded significant predictive performance, point estimates of prediction performance that exceeded chance levels under our null prediction model are overlaid ($p_{FDR} < .05$; see Figure S8 for empirical nulls and the Supplement for details). Point estimates that did not exceed chance levels are not shown. Significant predictive performance was only found for average controllability predicting positive psychosis spectrum symptoms, and this was observed for both RMSE and the correlation between true y and predicted y . *significant difference between connectivity features at $p_{FDR} < .05$. ac, average controllability; bc, betweenness centrality; cc, closeness centrality; FDR, false discovery rate-corrected; RMSE, root-mean-square error; sgc, subgraph centrality; str, strength.

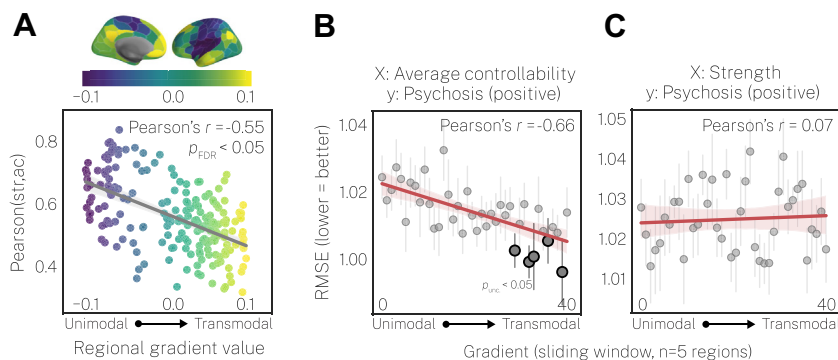


Figure 3. Average controllability and strength are less correlated in transmodal association cortex compared with unimodal cortex, and prediction performance for average controllability, not strength, is better in transmodal cortex. **(A)** The cross-subject Pearson's correlation between strength (str) and average controllability (ac) decreases as regions traverse up the principal cortical gradient. Thus, average controllability and strength show the greatest amount of unique variance in transmodal cortex. The p value of the spatial correlation between the principal gradient and the regional cross-subject correlation map was assigned via the spin test (62,64,66), using 10,000 spins. **(B, C)** Performance from our binned-regions prediction model (see Figure 1C and the Supplement for details) for

average controllability **(B)** and strength **(C)** predicting positive psychosis spectrum symptoms. Root-mean-squared error (RMSE) is presented as the mean over 10 stratified folds, and the vertical gray lines represent standard error over folds. Prediction performance for average controllability improved as a function of the cortical gradient, whereas strength did not. Thus, the best predictive performance of positive psychosis spectrum symptoms was observed for average controllability in association cortex. In addition, we tested the significance of predictive performance for each bin separately using our null prediction model. We found five bins located in the transmodal cortex for which prediction performance for average controllability exceeded chance levels ($p_{unc} < .05$; n , Nulls not shown). However, these effects were only observed at an uncorrected threshold of $p < .05$. This was likely due to the large number of multiple comparison corrections required to achieve false discovery rate (FDR)-corrected significance (80 tests, 1 per bin for each of strength and average controllability). We also note that the whole-brain model (see Figure 2 and Figure S8) was robustly significant and that there were fewer features used here for prediction by comparison (5 vs. 200).

average controllability (see Figure S11 for all $[X, y]$ combinations). Owing to the redundancy we observed between RMSE and accuracy in our whole-brain analyses, we focused on RMSE here. Specifically, we examined the extent to which RMSE varied as a function of the principal cortical gradient [see Figure S12 for RMSE as a function of the Yeo systems (65)]. As expected, for average controllability, we found prediction was better in transmodal cortex than in unimodal cortex (Figure 3B). We found no such relationship for strength (Figure 3C). These results were robust to bin size (Table S3). Thus, our results show a strong spatial component to the prediction of positive PS symptoms, wherein prediction is improved in transmodal cortex selectively for average controllability (Figure S11).

As an additional test of hypothesis 3, we recalculated average controllability, increasingly reducing its access to indirect connections by increasing the c parameter in equation 3 (see Supplement and Figure S3 for details). Figure 4A shows that increasingly restricting average controllability to indexing only direct connections resulted in stronger correlations with strength (y -axes) and diminishment of the spatial effect of the cortical gradient. Thus, not only do strength and average controllability become increasingly redundant at greater c , but their unique variance also becomes less differentiable as a function of the cortical hierarchy. Finally, the correlation between performance for our binned-regions prediction model and the cortical gradient also decreased at greater c (Figure 4B). Thus, average controllability's sensitivity to indirect structural connectivity is crucial to its superior predictive performance of positive PS symptoms.

DISCUSSION

A focus on examining interindividual variation in direct regional structural connectivity has generated an incomplete picture of the pathophysiology of the PS. Using NCT (9,43), we investigated the differential contributions of direct and indirect

properties of regional connectivity profiles to predict positive and negative PS symptoms. We found that average controllability better predicted positive PS symptoms compared with strength, while strength and average controllability predicted negative PS symptoms to a similar degree. Furthermore, while we observed differential predictive performance across betweenness, closeness, and subgraph centrality, only the pairing between average controllability and positive PS symptoms yielded above-chance predictive performance. This suggests that robust prediction of positive PS symptoms required characterization of both direct and indirect connectivity through NCT. In addition, we found that strength and average controllability exhibited the greatest amount of unique interindividual variance in transmodal cortex, and that this unique variance linked to improved predictive performance of positive PS symptoms for average controllability. Finally, we found that restricting average controllability's access to indirect connectivity reduced both the unique covariance with strength and the predictive performance in transmodal cortex, bringing both more in line with that observed in unimodal cortex. Overall, our results demonstrate that NCT can quantify and probe the complex indirect connectivity pathways that stem from transmodal cortex and that capturing this complexity can help understand positive PS symptoms.

Predicting Positive Psychosis Symptoms Using NCT

The structural connectivity correlates of the PS are increasingly well studied (32–40,66,67). Compared with graph-theoretic measures of connectivity, NCT has received relatively little attention; to our knowledge, only one previous study examined average controllability in bipolar disorder, reporting reductions compared with healthy control subjects (48). We found that indexing indirect connections through average controllability was able to significantly predict positive PS symptoms out-of-sample where strength and other graph-theoretic measures of centrality could not. Furthermore,

Network Controllability Predicts the Psychosis Spectrum

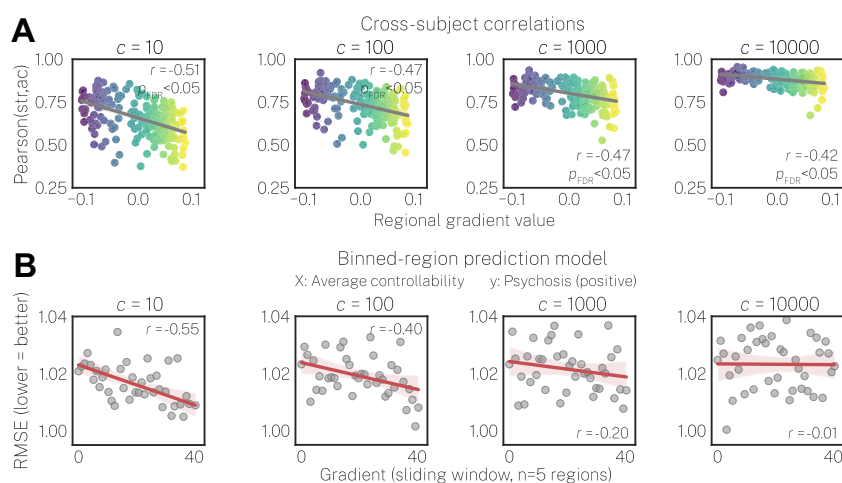


Figure 4. Restricting average controllability to direct structural connections increases redundancy with strength and reduces prediction performance in transmodal cortex. Columns represent average controllability recalculated using different values of the c parameter from equation 3; greater values of c correspond to greater restriction of average controllability's capacity to access indirect connections (see Supplement and Figure S3 for details). **(A)** The cross-subject correlation between strength (str) and average controllability (ac) as a function of the principal cortical gradient. Increases in c resulted in increases to the cross-subject correlations (y-axes) and a reduction in the spatial correlations with the cortical gradient, wherein correlations in transmodal cortex became increasingly redundant. **(B)** Performance for the binned-regions prediction model for average controllability predicting positive psychosis spectrum symptoms. The spatial correlation between prediction performance and the

cortical gradient diminished with increasing c , yielding lower prediction performance in transmodal cortex. FDR, false discovery rate-corrected; RMSE, root-mean-squared error.

consistent with literature implicating hub dysconnectivity in schizophrenia (35), we found that average controllability showed better predictive performance of positive PS symptoms in transmodal association cortex compared with unimodal sensorimotor cortex. While simple structural connectivity features such as strength are readily interpretable from a network perspective, they lack an explicit model of macroscale brain function (68). Furthermore, while other metrics apart from average controllability exist that also capture indirect connections (17), some of which were studied here, many of them similarly lack an explicit model of brain dynamics. By contrast, average controllability models a region's capacity to distribute input energy throughout the brain to drive changes in brain state (9), facilitating the capacity to predict the brainwide response to external stimulation (10,69). Hence, our results demonstrate that the continued examination of NCT has potential implications for clinical treatment. For instance, external neurostimulation techniques, such as transcranial magnetic stimulation, are increasingly being investigated as treatment modalities for PS-related conditions, and candidate stimulation sites typically occupy transmodal cortex (70,71). Indeed, the analysis of neurostimulation data with NCT has begun to show promise (56).

Predicting Negative PS Symptoms

In contrast to positive PS symptoms, we found that betweenness and closeness centrality were the best predictors of negative PS symptoms. This suggests that the way in which we summarize indirect aspects of regional connectivity matters for the prediction of different PS dimensions. However, our null prediction model revealed no significant prediction effects for psychosis-negative scores, suggesting that we were unable to predict negative PS symptoms with any connectivity feature beyond chance levels. This failure may be due to the fact that in our model, the psychosis-negative factor explained less variance in symptom data compared with the psychosis-positive factor (Table S1). Hence, our estimate of negative

PS symptoms was perhaps noisier than our estimate of positive PS symptoms. Similar disparities in variance explained between positive and negative psychosis dimensions have also been reported in previous literature (72). Thus, future work improving the modeling of variance in negative PS symptoms is needed and may yield improved predictive performance in brain-based association studies.

Analysis of Indirect Connectivity Is Crucial in Transmodal Cortex

Analysis of the principal cortical gradient (25) revealed that the cross-subject correlations between strength and average controllability were lowest in transmodal cortex. While previous research has demonstrated that high average controllability depends on high strength (9), to our knowledge, our study is the first to illustrate that interindividual covariance between these features has a strong spatial component. This result is consistent with the idea that brain regions' structural properties, and potential strategies for affecting change in functional activity and connectivity, vary markedly over the cortical hierarchy (28,73–82). For instance, work in rodents illustrates that transmodal cortex broadly occupies the topmost level of the cortical hierarchy (30), wherein regions exert regulatory control over the lower levels through cascading sets of feedback projections. These differential roles across the mouse cortical hierarchy are also reflected by distinct microstructural properties, including variations to gene expression and cytoarchitecture (83). In human work, top-down connections from association cortex enable more efficient distribution of activity across the human brain relative to sensorimotor cortex (28). Thus, our results suggest that compared with strength and the other centrality measures studied herein, average controllability is more sensitive to these cascading circuits of connectivity. Indeed, we found that reducing average controllability's access to indirect connections both increased the correlation with strength and reduced the spatial dependence of these correlations on the cortical gradient. Our results illustrate the

value of using NCT to supplement the analysis of interindividual differences in structural connectivity, particularly in transmodal association cortex.

Limitations

A limitation of this study is the use of a linear model of neuronal dynamics to estimate average controllability. While this assumption is an oversimplification of brain dynamics, linear models explain variance in the slow fluctuations in brain activity recorded by functional magnetic resonance imaging (44,84), suggesting that they approximate the kinds of data commonly used to examine brain function in psychiatry. An additional limitation was our measurement of negative PS symptoms, which had limited construct coverage compared with our measurement of positive PS symptoms (52), thus potentially impeding our prediction efforts. Future work could use dedicated instruments for assessing negative PS symptoms such as the Clinical Assessment Interview for Negative Symptoms (85).

Conclusions

Our results suggest that the dysconnectivity in transmodal cortex associated with positive PS symptoms reflects more than just disruptions to the direct connections among regions, and that understanding dysconnectivity along longer indirect pathways, particularly via NCT, is critical to out-of-sample prediction. More broadly, our results highlight the advantages of using model-based approaches to networks such as NCT to understand dimensions of psychopathology. Continued examination of NCT and related approaches may facilitate improved predictive modeling in computational psychiatry, a goal critical to driving the field toward personalized medicine.

ACKNOWLEDGMENTS AND DISCLOSURES

This study was supported by the National Institute of Mental Health (Grant Nos. R21MH106799 [to DSB and TDS], R01MH113550 [to TDS and DSB], and RF1MH116920 [to TDS and DSB]) and the Swartz Foundation. Additional support was provided by Grant No. R01MH120482 (to TDS), R01MH107703 (to TDS), the John D. and Catherine T. MacArthur Foundation (to DSB), the Army Research Office contracts (W911NF-14-1-0679 and W911NF-16-1-0474 [to DSB]), the Army Research Laboratory contract (W911NF-10-2-0022 [to DSB]), Grant Nos. R01MH107235 (to RCG), R01MH119219 (to RCG and REG), R01MH119185 (to DRR), R01MH120174 (to DRR), R01MH113565 (to DHW), and the Penn-CHOP Lifespan Brain Institute. The PNC was supported by Grant Nos. RC2MH089983 and RC2MH089924.

We thank Jason Z. Kim, Dr. Jennifer Stiso, and Dr. Eli Cornblath for valuable discussions during the writing of the manuscript.

Citation Diversity Statement: Recent work in several fields of science has identified a bias in citation practices such that papers from women and other minority scholars are undercited relative to the number of such papers in the field (86–90). Here, we sought to proactively consider choosing references that reflect the diversity of the field in thought, form of contribution, gender, race, ethnicity, and other factors. First, we obtained the predicted gender of the first and last author of each reference by using databases that store the probability of a first name being carried by a woman (90,91). By this measure (and excluding self-citations to the first and last authors of our current paper), our references contain 10.67% woman (first)/woman (last), 11.16% man/woman, 17.84% woman/man, and 60.33% man/man. This method is limited in that 1) names, pronouns, and social media profiles used to construct the databases may not, in every case, be indicative of gender identity, and 2) it cannot account for intersex, nonbinary, or transgender people. Second, we obtained predicted racial/ethnic category of the first

and last author of each reference by databases that store the probability of a first and last name being carried by an author of color (92,93). By this measure (and excluding self-citations), our references contain 12.43% author of color (first)/author of color (last), 18.54% white author/author of color, 17.64% author of color/white author, and 51.39% white author/white author. This method is limited in that 1) names and Wikipedia profiles used to make the predictions may not be indicative of racial/ethnic identity, and 2) it cannot account for Indigenous and mixed-race authors, or those who may face differential biases due to the ambiguous racialization or ethnicization of their names. We look forward to future work that could help us to better understand how to support equitable practices in science.

The authors report no biomedical financial interests or potential conflicts of interest.

ARTICLE INFORMATION

From the Department of Bioengineering (LP, DSB), School of Engineering & Applied Science; Department of Electrical & Systems Engineering (DSB), School of Engineering & Applied Science; Department of Physics & Astronomy (DSB), College of Arts & Sciences, University of Pennsylvania; Department of Psychiatry (TMM, MEC, MC, DRR, DHW, RCG, REG, TDS, DSB), Perelman School of Medicine, University of Pennsylvania; Lifespan Brain Institute (TMM, MEC, MC, DRR, DHW, RCG, REG, TDS), University of Pennsylvania & Children's Hospital of Philadelphia; Center for Biomedical Image Computing and Analytics (MC, DHW, TDS), Department of Neurology (RCG, REG, DSB), and Department of Radiology (RCG, REG), Perelman School of Medicine, Philadelphia, Pennsylvania; and Santa Fe Institute (DSB), Santa Fe, New Mexico.

Address correspondence to Danielle S. Bassett, Ph.D., at dsb@seas.upenn.edu.

Received Sep 30, 2020; revised Feb 11, 2021; accepted Mar 15, 2021.

Supplementary material cited in this article is available online at <https://doi.org/10.1016/j.biopsych.2021.03.016>.

REFERENCES

- Owen MJ, Sawa A, Mortensen PB (2016): Schizophrenia. *Lancet* 388:86–97.
- Paus T, Keshavan M, Giedd JN (2008): Why do many psychiatric disorders emerge during adolescence? *Nat Rev Neurosci* 9:947–957.
- Grant P, Green MJ, Mason OJ (2018): Models of schizotypy: The importance of conceptual clarity. *Schizophr Bull* 44:S556–S563.
- Nath M, Wong TP, Srivastava LK (2021): Neurodevelopmental insights into circuit dysconnectivity in schizophrenia. *Prog Neuro-psychopharmacol Biol Psychiatry* 104:110047.
- van den Heuvel MP, Sporns O (2019): A cross-disorder connectome landscape of brain dysconnectivity. *Nat Rev Neurosci* 20:435–446.
- Bassett DS, Xia CH, Satterthwaite TD (2018): Understanding the emergence of neuropsychiatric disorders with network neuroscience. *Biol Psychiatry Cogn Neurosci Neuroimaging* 3:742–753.
- Fornito A, Zalesky A, Breakspear M (2015): The connectomics of brain disorders. *Nat Rev Neurosci* 16:159–172.
- Avena-Koenigsberger A, Yan X, Kolchinsky A, van den Heuvel MP, Hagmann P, Sporns O (2019): A spectrum of routing strategies for brain networks. *PLoS Comput Biol* 15:e1006833.
- Gu S, Pasqualetti F, Cieslak M, Telesford QK, Yu AB, Kahn AE, et al. (2015): Controllability of structural brain networks. *Nat Commun* 6:8414.
- Muldoon SF, Pasqualetti F, Gu S, Cieslak M, Grafton ST, Vettel JM, Bassett DS (2016): Stimulation-based control of dynamic brain networks. *PLoS Comput Biol* 12:e1005076.
- Srivastava P, Nozari E, Kim JZ, Ju H, Zhou D, Becker C, et al. (2020): Models of communication and control for brain networks: Distinctions, convergence, and future outlook. *Netw Neurosci* 4:1122–1159.
- Saggio ML, Ritter P, Jirsa VK (2016): Analytical operations relate structural and functional connectivity in the brain. *PLoS One* 11:e0157292.
- Bansal K, Garcia JO, Tompson SH, Verstynen T, Vettel JM, Muldoon SF (2019): Cognitive chimera states in human brain networks. *Sci Adv* 5:eaau8535.

Network Controllability Predicts the Psychosis Spectrum

14. Hövel P, Viol A, Loske P, Merfort L, Vuksanović V (2020): Synchronization in functional networks of the human brain. *J Nonlinear Sci* 30:2259–2282.
15. Schirner M, McIntosh AR, Jirsa V, Deco G, Ritter P (2018): Inferring multi-scale neural mechanisms with brain network modelling. *Elife* 7: e28927.
16. Rubinov M, Sporns O (2010): Complex network measures of brain connectivity: Uses and interpretations. *Neuroimage* 52:1059–1069.
17. Oldham S, Fulcher B, Parkes L, Arnatkevič I, A, Suo C, Fornito A (2019): Consistency and differences between centrality measures across distinct classes of networks. *PLoS One* 14:e0220061.
18. Dennis EL, Thompson PM (2013): Typical and atypical brain development: A review of neuroimaging studies. *Clin Res* 15:359–384.
19. Baker ST, Lubman DI, Yücel M, Allen NB, Whittle S, Fulcher BD, *et al.* (2015): Developmental changes in brain network hub connectivity in late adolescence. *J Neurosci* 35:9078–9087.
20. Oldham S, Fornito A (2019): The development of brain network hubs. *Dev Cogn Neurosci* 36:100607.
21. Sporns O, Honey CJ, Kötter R (2007): Identification and classification of hubs in brain networks. *PLoS One* 2:e1049.
22. van den Heuvel MP, Sporns O (2013): Network hubs in the human brain. *Trends Cogn Sci* 17:683–696.
23. Buckner RL, Sepulcre J, Talukdar T, Krienen FM, Liu H, Hedden T, *et al.* (2009): Cortical hubs revealed by intrinsic functional connectivity: Mapping, assessment of stability, and relation to Alzheimer's disease. *J Neurosci* 29:1860–1873.
24. Buckner RL, Krienen FM (2013): The evolution of distributed association networks in the human brain. *Trends Cogn Sci* 17:648–665.
25. Margulies DS, Ghosh SS, Goulas A, Falkiewicz M, Huntenburg JM, Langs G, *et al.* (2016): Situating the default-mode network along a principal gradient of macroscale cortical organization. *Proc Natl Acad Sci U S A* 113:12574–12579.
26. Smallwood J, Karapanagiotidis T, Ruby F, Medea B, de Caso I, Konishi M, *et al.* (2016): Representing representation: Integration between the temporal lobe and the posterior cingulate influences the content and form of spontaneous thought. *PLoS One* 11: e0152272.
27. Bertolero MA, Yeo BTT, Bassett DS, D'Esposito M (2018): A mechanistic model of connector hubs, modularity and cognition. *Nat Hum Behav* 2:765–777.
28. Misić B, Betzel RF, Nematzadeh A, Goñi J, Griffa A, Hagmann P, *et al.* (2015): Cooperative and competitive spreading dynamics on the human connectome. *Neuron* 86:1518–1529.
29. Vázquez-Rodríguez B, Liu Z-Q, Hagmann P, Misić B (2020): Signal propagation via cortical hierarchies. *Netw Neurosci* 4:1072–1090.
30. Harris JA, Mihalas S, Hirokawa KE, Whitesell JD, Choi H, Bernard A, *et al.* (2019): Hierarchical organization of cortical and thalamic connectivity. *Nature* 575:195–202.
31. Bazinet V, Vos de Wael R, Hagmann P, Bernhardt BC, Misić B (2020): Multiscale communication in cortico-cortical networks. *bioRxiv*. <https://doi.org/10.1101/2020.10.02.323030>.
32. Canu E, Agosta F, Filippi M (2015): A selective review of structural connectivity abnormalities of schizophrenic patients at different stages of the disease. *Schizophr Res* 161:19–28.
33. Fitzsimmons J, Kubicki M, Shenton ME (2013): Review of functional and anatomical brain connectivity findings in schizophrenia. *Curr Opin Psychiatry* 26:172–187.
34. Griffa A, Baumann PS, Klauser P, Mullier E, Cleusix M, Jenni R, *et al.* (2019): Brain connectivity alterations in early psychosis: from clinical to neuroimaging staging. *Transl Psychiatry* 9:62.
35. Klauser P, Baker ST, Cropley VL, Bousman C, Fornito A, Cocchi L, *et al.* (2017): White matter disruptions in schizophrenia are spatially widespread and topologically converge on brain network hubs. *Schizophr Bull* 43:425–435.
36. Narr KL, Leaver AM (2015): Connectome and schizophrenia. *Curr Opin Psychiatry* 28:229–235.
37. Rubinov M, Bullmore E (2013): Schizophrenia and abnormal brain network hubs. *Clin Res* 15:339–349.
38. van den Heuvel MP, Mandl RCW, Stam CJ, Kahn RS, Hulshoff Pol HE (2010): Aberrant frontal and temporal complex network structure in schizophrenia: A graph theoretical analysis. *J Neurosci* 30:15915–15926.
39. van den Heuvel MP, Sporns O, Collin G, Scheewe T, Mandl RCW, Cahn W, *et al.* (2013): Abnormal rich club organization and functional brain dynamics in schizophrenia. *JAMA Psychiatry* 70:783–792.
40. Wang Q, Su TP, Zhou Y, Chou KH, Chen IY, Jiang T, Lin CP (2012): Anatomical insights into disrupted small-world networks in schizophrenia. *Neuroimage* 59:1085–1093.
41. Alexander-Bloch AF, Gogtay N, Meunier D, Birn R, Clasen L, Lalonde F, *et al.* (2010): Disrupted modularity and local connectivity of brain functional networks in childhood-onset schizophrenia. *Front Syst Neurosci* 4:147.
42. van den Heuvel MP, Fornito A (2014): Brain networks in schizophrenia. *Neuropsychol Rev* 24:32–48.
43. Karrer TM, Kim JZ, Stiso J, Kahn AE, Pasqualetti F, Habel U, Bassett DS (2020): A practical guide to methodological considerations in the controllability of structural brain networks. *J Neural Eng* 17: 026031.
44. Nozari E, Stiso J, Caciagli L, Cornblath EJ, He X, Bertolero MA, *et al.*: Is the brain macroscopically linear? A system identification of resting state dynamics (2020). *arXiv* <http://arxiv.org/abs/2012.12351>.
45. Tang E, Giusti C, Baum GL, Gu S, Pollock E, Kahn AE, *et al.* (2017): Developmental increases in white matter network controllability support a growing diversity of brain dynamics. *Nat Commun* 8:1252.
46. Cornblath EJ, Tang E, Baum GL, Moore TM, Adebimpe A, Roalf DR, *et al.* (2019): Sex differences in network controllability as a predictor of executive function in youth. *Neuroimage* 188:122–134.
47. Cui Z, Stiso J, Baum GL, Kim JZ, Roalf DR, Betzel RF, *et al.* (2020): Optimization of energy state transition trajectory supports the development of executive function during youth. *eLife* 9:e53060.
48. Jeganathan J, Perry A, Bassett DS, Roberts G, Mitchell PB, Breakspear M (2018): Fronto-limbic dysconnectivity leads to impaired brain network controllability in young people with bipolar disorder and those at high genetic risk. *Neuroimage Clin* 19:71–81.
49. Parkes L, Moore TM, Calkins ME, Cook PA, Cieslak M, Roalf DR, *et al.* (2021): Transdiagnostic dimensions of psychopathology explain individuals' unique deviations from normative neurodevelopment in brain structure. *Transl Psychiatry* 11:232.
50. Satterthwaite TD, Elliott MA, Ruparel K, Loughhead J, Prabhakaran K, Calkins ME, *et al.* (2014): Neuroimaging of the Philadelphia neurodevelopmental cohort. *Neuroimage* 86:544–553.
51. Calkins ME, Moore TM, Merikangas KR, Burstein M, Satterthwaite TD, Bilker WB, *et al.* (2014): The psychosis spectrum in a young U.S. community sample: Findings from the Philadelphia neurodevelopmental cohort. *World Psychiatry* 13:296–305.
52. Calkins ME, Merikangas KR, Moore TM, Burstein M, Behr MA, Satterthwaite TD, *et al.* (2015): The Philadelphia neurodevelopmental Cohort: Constructing a deep phenotyping collaborative. *J Child Psychol Psychiatry* 56:1356–1369.
53. Moore TM, Calkins ME, Satterthwaite TD, Roalf DR, Rosen AFG, Gur RC, Gur RE (2019): Development of a computerized adaptive screening tool for overall psychopathology (“p”). *J Psychiatr Res* 116:26–33.
54. Schaefer A, Kong R, Gordon EM, Laumann TO, Zuo XN, Holmes AJ, *et al.* (2018): Local-global parcellation of the human cerebral cortex from intrinsic functional connectivity MRI. *Cereb Cortex* 28:3095–3114.
55. Pasqualetti F, Zampieri S, Bullo F (2014): Controllability metrics, limitations and algorithms for complex networks. *American Control Conference*, 3287–3292.
56. Stiso J, Khambhati AN, Menara T, Kahn AE, Stein JM, Das SR, *et al.* (2019): White matter network architecture guides direct electrical stimulation through optimal state transitions. *Cell Rep* 28:2554–2566.e7.
57. Betzel RF, Gu S, Medaglia JD, Pasqualetti F, Bassett DS (2016): Optimally controlling the human connectome: The role of network topology. *Sci Rep* 6:30770.

58. Yan G, Vértes PE, Towilson EK, Chew YL, Walker DS, Schafer WR, Barabási AL (2017): Network control principles predict neuron function in the *Caenorhabditis elegans* connectome. *Nature* 550:519–523.
59. Glahn DC, Winkler AM, Kochunov P, Almasy L, Duggirala R, Carless MA, *et al.* (2010): Genetic control over the resting brain. *Proc Natl Acad Sci U S A* 107:1223–1228.
60. Valk SL, Hoffstaedter F, Camilleri JA, Kochunov P, Yeo BTT, Eickhoff SB (2020): Personality and local brain structure: Their shared genetic basis and reproducibility. *Neuroimage* 220:117067.
61. Murphy KP (2012): *Machine Learning: A Probabilistic Perspective*. Cambridge, MA: MIT Press.
62. Váša F, Seidlitz J, Romero-Garcia R, Whitaker KJ, Rosenthal G, Vértes PE, *et al.* (2018): Adolescent tuning of association cortex in human structural brain networks. *Cereb Cortex* 28:281–294.
63. Alexander-Bloch A, Raznahan A, Bullmore E, Giedd J (2013): The convergence of maturational change and structural covariance in human cortical networks. *J Neurosci* 33:2889–2899.
64. Alexander-Bloch AF, Shou H, Liu S, Satterthwaite TD, Glahn DC, Shinohara RT, *et al.* (2018): On testing for spatial correspondence between maps of human brain structure and function. *Neuroimage* 178:540–551.
65. Yeo BTT, Krienen FM, Sepulcre J, Sabuncu MR, Lashkari D, Hollinshead M, *et al.* (2011): The organization of the human cerebral cortex estimated by intrinsic functional connectivity. *J Neurophysiol* 106:1125–1165.
66. Oestreich LKL, Randeniya R, Garrido MI (2019): White matter connectivity reductions in the pre-clinical continuum of psychosis: A connectome study. *Hum Brain Mapp* 40:529–537.
67. Vijayakumar N, Bartholomeusz C, Whitford T, Hermens DF, Nelson B, Rice S, *et al.* (2016): White matter integrity in individuals at ultra-high risk for psychosis: A systematic review and discussion of the role of polyunsaturated fatty acids. *BMC Psychiatry* 16:287.
68. Bassett DS, Sporns O (2017): Network neuroscience. *Nat Neurosci* 20:353–364.
69. Tang E, Bassett DS (2018): Colloquium: Control of dynamics in brain networks. *Rev Mod Phys* 90:031003.
70. Lefaucheur JP, André-Obadia N, Antal A, Ayache SS, Baeken C, Benninger DH, *et al.* (2014): Evidence-based guidelines on the therapeutic use of repetitive transcranial magnetic stimulation (rTMS). *Clin Neurophysiol* 125:2150–2206.
71. Cole JC, Green Bernacki C, Helmer A, Pinninti N, O'reardon JP (2015): Efficacy of transcranial magnetic stimulation (TMS) in the treatment of schizophrenia: A review of the literature to date. *Innov Clin Neurosci* 12:12–19.
72. Sabaroedin K, Tiego J, Parkes L, Sforazzini F, Finlay A, Johnson B, *et al.* (2019): Functional connectivity of corticostriatal circuitry and psychosis-like experiences in the general community. *Biol Psychiatry* 86:16–24.
73. Shafiei G, Markello RD, Vos de Wael R, Bernhardt BC, Fulcher BD, Misis B (2020): Topographic gradients of intrinsic dynamics across neocortex. *ELife* 9:e62116.
74. Suárez LE, Markello RD, Betzel RF, Misis B (2020): Linking structure and function in macroscale brain networks. *Trends Cogn Sci* 24:302–315.
75. Vázquez-Rodríguez B, Suárez LE, Markello RD, Shafiei G, Paquola C, Hagmann P, *et al.* (2019): Gradients of structure–function tethering across neocortex. *Proc Natl Acad Sci U S A* 116:21219–21227.
76. Demirtaş M, Burt JB, Helmer M, Ji JL, Adkinson BD, Glasser MF, *et al.* (2019): Hierarchical heterogeneity across human cortex shapes large-scale neural dynamics. *Neuron* 101:1181–1194.e13.
77. Baum GL, Cui Z, Roalf DR, Ciric R, Betzel RF, Larsen B, *et al.* (2020): Development of structure-function coupling in human brain networks during youth. *Proc Natl Acad Sci U S A* 117:771–778.
78. Fallon J, Ward PGD, Parkes L, Oldham S, Arnatkevičiūtė A, Fornito A, Fulcher BD (2020): Timescales of spontaneous fMRI fluctuations relate to structural connectivity in the brain. *Network Neurosci* 4:788–806.
79. Goñi J, van den Heuvel MP, Avena-Koenigsberger A, Velez de Mendizabal N, Betzel RF, Griffa A, *et al.* (2014): Resting-brain functional connectivity predicted by analytic measures of network communication. *Proc Natl Acad Sci U S A* 111:833–838.
80. Seguin C, Razi A, Zalesky A (2019): Inferring neural signalling directionality from undirected structural connectomes. *Nat Commun* 10:4289.
81. Seguin C, Tian Y, Zalesky A (2020): Network communication models improve the behavioral and functional predictive utility of the human structural connectome. *Netw Neurosci* 4:980–1006.
82. Abdelnour F, Voss HU, Raj A (2014): Network diffusion accurately models the relationship between structural and functional brain connectivity networks. *Neuroimage* 90:335–347.
83. Fulcher BD, Murray JD, Zerbi V, Wang XJ (2019): Multimodal gradients across mouse cortex. *Proc Natl Acad Sci U S A* 116:4689–4695.
84. Cornblath EJ, Ashourvan A, Kim JZ, Betzel RF, Ciric R, Adebimpe A, *et al.* (2020): Temporal sequences of brain activity at rest are constrained by white matter structure and modulated by cognitive demands. *Commun Biol* 3:261.
85. Kring AM, Gur RE, Blanchard JJ, Horan WP, Reise SP (2013): The clinical assessment interview for negative symptoms (CAINS): Final development and validation. *Am J Psychiatry* 170:165–172.
86. Mitchell SM, Lange S, Brus H (2013): Gendered citation patterns in international relations journals. *Int Stud Perspect* 14:485–492.
87. Maliniak D, Powers R, Walter BF (2013): The gender citation gap in international relations. *Int Organ* 67:889–922.
88. Caplar N, Tacchella S, Birrer S (2017): Quantitative evaluation of gender bias in astronomical publications from citation counts. *Nat Astron* 1:0141.
89. Dion ML, Sumner JL, Mitchell SM (2018): Gendered citation patterns across political science and social science methodology fields. *Polit Anal* 26:312–327.
90. Dworkin JD, Linn KA, Teich EG, Zurn P, Shinohara RT, Bassett DS (2020): The extent and drivers of gender imbalance in neuroscience reference lists. *Nat Neurosci* 23:918–926.
91. Zhou D, Cornblath EJ, Stiso J, Teich EG, Dworkin JD, Blevins AS, Bassett DS: Gender Diversity Statement and Code Notebook v1.0. Zenodo. Available at: <https://doi.org/10.5281/zenodo.3672110>. Accessed September 29, 2020.
92. Ambekar A, Ward C, Mohammed J, Male S, Skiena S (2009): Name-ethnicity classification from open sources; Proceedings of KDD'09: The 15th ACM SIGKDD International Conference on Knowledge Discovery and Data Mining, June 28–July 1, Paris, France.
93. Sood G, Laohaprapanon S (2018): Predicting race and ethnicity From the sequence of characters in a name. arXiv doi: <http://arxiv.org/abs/1805.02109>.